Supporting Information

Bridging Hydrometallurgy and Biochemistry: A Protein-based Process for Recovery and Separation of Rare Earth Elements

Ziye Dong[1], Joseph A. Mattocks[2], Gauthier J.-P. Deblonde[1,3], Dehong Hu[4], Yongqin Jiao,[1] Joseph A. Cotruvo, Jr.[2*], Dan M. Park[1*]

[1]*Physical and Life Sciences Directorate, Lawrence Livermore National Laboratory, Livermore, California 94550, United States*

[2]*Department of Chemistry, The Pennsylvania State University, University Park, Pennsylvania 16802, United States*

[3]*Glenn T. Seaborg Institute, Lawrence Livermore National Laboratory, Livermore, California 94550, United States*

[4]*Environmental Molecular Sciences Laboratory, Pacific Northwest National Laboratory, Richland, Washington 99354, United States*

Corresponding authors: juc96@psu.edu (J.A.C.); park36@llnl.gov (D.M.P.)

This file contains methods, supplementary results, supplementary Tables S1-8, supplementary Figures S1-6, and supplementary References.

METHODS

Note: No unexpected or unusually high safety hazards were encountered.

Chemicals and materials

REE chloride salts (> 99.9%), solvents, and buffers were purchased from Millipore Sigma. Amine-functionalized agarose beads were purchased from Nanocs Inc. *N*-Succinimidyl 4-(maleimidomethyl) cyclohexane-1-carboxylate (SMCC) was purchased from Chem-Impex International, Inc. and used without further purification. NHS-Fluorescein (5/6-carboxyfluorescein succinimidyl ester), mixed isomer, was purchased from ThermoFisher Scientific.

Preparation of LanM

The plasmid containing the gene encoding for LanM-GSGC was obtained from Twist Bioscience (pET-29b(+)-LanM-GSGC). The gene sequence consisted of the codon-optimized wt-LanM sequence with (ggcagcggctgc) inserted immediately 5' to the stop codon.[1] The protein was overexpressed in *E. coli* BL21(DE3) cells (NEB) at 37 °C after induction with 0.2 mM IPTG at an OD_{600nm} of 0.6. Purification was carried out as described except all buffers contained 5 mM TCEP.[2] Briefly, cells were lysed and loaded to a 25-mL (2.5 × 5 cm) Q-Sepharose Fast Flow column and eluted using a 0.01 – 1 M NaCl gradient. LanM-GSGC containing fractions were purified further using gel filtration chromatography (HiLoad 16/600 Superdex 75 pg column in 30 mM MOPS, 100 mM KCl, 5 mM $CaCl_2$, 5% glycerol, 5 mM TCEP, pH 7.0). LanM-GSGC-containing fractions were exchanged by FPLC into 20 mM acetate, 10 mM EDTA, 100 mM NaCl, 5% glycerol, pH 4.0, concentrated to ~3 mM, and frozen in liquid N_2.

Spectrofluorometric titrations of wt-LanM

A solution of 20 μM Chelex-treated LanM was prepared in 20 mM acetate, 100 mM KCl, pH 5.0. In experiments that began with metalated LanM, 40 μM (2 equivalents) of metal was also added. The protein solution (600 μL) was placed in a 10-mm quartz spectrofluorometry cuvette (Starna Cells, 18F-Q-10-GL14-S) and assayed using a PerkinElmer fluorescence spectrometer FL 6500 in kinetic mode (80 kW power, 278 nm excitation, 2.5 nm excitation slit width, 307 nm emission, 5 nm emission slit width). Titrations were carried out through addition of at least 0.6 μL of titrant (either 10 mM metal or 1 mM citrate, pH 5.0) followed by ~1 min of signal equilibration. For each data point, 10 s of signal were averaged after equilibration. These values were corrected for dilution and normalized to $F_{307nm} = 1$ for the apoprotein. Each experiment was performed in triplicate.

Maleimide functionalization of agarose beads

Amine-functionalized agarose microbeads (1.2 mL) were transferred into a 5 mL Eppendorf tube and washed with pH 7.4 phosphate-buffered saline (PBS) three times and resuspended at a final volume of ~ 1.7 mL (1.2 mL microbeads and 0.5 mL PBS supernatant). SMCC (0.15 g) was dissolved in 3.4 mL DMSO and combined with the microbeads. After 2.5 h incubation on a rocker mixer at room temperature, the functionalized agarose microbeads were washed with DMSO three times to remove unreacted SMCC and then washed with coupling buffer (50 mM HEPES, 50 mM KCl, and 10 mM ethylenediaminetetraacetic acid (EDTA), pH 7) three times to remove DMSO solvent. The maleimide-microbeads were then used for LanM immobilization within 2 h.

LanM immobilization

LanM immobilization was carried out using a thiol-maleimide conjugation reaction. Specifically, immediately before immobilization, LanM-GSGC was exchanged into the coupling buffer using VivaSpin® 2 centrifugal concentrators (molecular weight cut-off 3,000 Da, GE Healthcare), which yielded a final protein concentration of ~ 2 mM. Then 2 mL of LanM solution was combined with 1 mL of maleimide-microbeads and the conjugation reaction was run for 16 h at room temperature. Unconjugated LanM was removed by washing with coupling buffer and the LanM-microbeads were stored in coupling buffer for subsequent tests. The maleimide-microbeads were also incubated with coupling buffer without LanM protein as an unconjugated control sample. To quantify LanM immobilization yield, Pierce™ BCA Protein Assay (ThermoFisher Scientific) was used to determine the LanM concentration in the reaction solution before and after the conjugation reaction. Briefly, a working solution was made by combining Reagent A and Reagent B at a 1:8 ratio. Working solution (200 µL) and 10 µL of sample (protein) were added to each well, respectively. Samples containing more than 2000 µg/mL protein were pre-diluted with coupling buffer. The 96-well plate was then shaken at 300 rpm for 30 s on a plate shaker, followed by 30 min incubation at 37 °C. After cooling the plate to room temperature, absorbance at 562 nm was measured and compared to BSA standards. In control experiments, it was shown that 2.0 mg/mL LanM gives the same assay response as 1.0 mg/mL BSA. Similarly, LanM immobilization kinetics were determined by monitoring the depletion of LanM protein in the reaction solution. The LanM concentration in the reaction solution at 6 min, 1 h, 3 h and 15 h after the start of conjugation reaction was measured in triplicate.

Fourier transform infrared (FTIR)

Fourier transform infrared (FTIR) spectra were recorded with a Cary 630 FTIR spectrometer (Agilent Technologies, USA) using a diamond-ATR sample module. Each acquisition was the average of 64 scans (650 - 4000 cm^{-1}) and was background corrected.

LanM labelling with fluorescein

LanM (0.3 mL, 2 mM) was exchanged into 4-(2-hydroxyethyl)-1-piperazineethanesulfonic acid (HEPES) buffer (10 mM; pH 7) with 100 mM KCl and 8 mM Nd^{3+} using a spin column (Zeba™ Spin Desalting Columns, 7K MWCO, ThermoFisher Scientific). Fluorescein NHS ester (1 mg) was dissolved in dimethyl sulfoxide (DMSO, 30 μL) and added into the LanM solution at ~ 3 mg/mL final concentration. After a 3 h incubation at room temperature, the untagged dyes were removed using a spin column (Zeba™ Spin Desalting Columns, 7K MWCO, ThermoFisher Scientific).

Confocal Microscopy

For confocal microscopy, fluorescein labeled LanM was used for immobilization on agarose microbeads. The microbeads were then dropped onto a microscope glass coverslip. The samples were imaged by a Zeiss LSM 710 confocal microscope equipped with a 10X NA 0.3 objective. A 488 nm wavelength laser was used to excite the fluorescein in the microbeads. 3-dimensional fluorescence images and bright-field images were acquired simultaneously.

Breakthrough column experiments

Econo-Column glass chromatography columns (Bio-Rad; 5 cm × 0.5 cm) were filled with MilliQ water (18.2 MΩ cm^{-1}) and then LanM-microbeads were added gravimetrically. Columns were washed with 25 mM HCl, MilliQ water, and conditioned with buffer solution (same buffer for

breakthrough experiment, see below) before conducting breakthrough experiments. REE stock solutions were prepared by dissolving individual REE chloride salts in 1 mM HCl. The stock solutions were diluted either in 10 mM buffer (pH 5: Homopiperazine-1,4-bis(2-ethanesulfonic acid, Homo-PIPES); pH 4: acetate acid; pH 3.5 – 2.2: glycine) or HCl at the desired pH. The REE solutions were pumped at 0.5 mL/min unless otherwise specified and the column effluent was collected in 1.0 mL aliquots. A washing step with 5 bed volumes of MilliQ water was included before performing desorption experiments. For single REE ion solutions, REE ion concentrations were quantified by Arsenazo III assay. Specifically, 40 μL of sample was combined with 40 μL of 12.5 wt.% trichloroacetic acid (TCA) and then added to 120 μL of filtered 0.1 wt.% Arsenazo in 6.25 wt.% TCA. Absorbance at 652 nm was measured and compared to standards to determine the REE metal ion concentrations. The accuracy of the colorimetric assay was also confirmed in our previous work by ICP-MS.[3] For experiments with REE mixtures or leachates, the metal ion concentrations were determined by ICP-MS.

For the REE pair separation experiments, the metal ion purity is defined as:

$$Purity_{REE1} = \frac{C_{REE1}}{C_{REE1} + C_{REE2}}$$

where C_{REE1} and C_{REE2} are molar concentration of REE1 and REE2, respectively.

The purification factor β_{ij} is defined as:

$$\beta_{ij} = \frac{Y_i/Y_j}{X_i/X_j}$$

where Y_i and Y_j are molar concentration of metal ions i and j in eluent, respectively, and X_i and X_j are molar concentration of metal ions i and j in feed, respectively.

Inductively coupled plasma mass spectrometry (ICP-MS)

The elemental composition of solutions was measured by ICP-MS as previously described.[4, 5] The elemental composition of the multi-element (non-REE and Nd; Nd/Y) synthetic solutions and leachate solutions were determined using an Thermo Fisher Scientific iCAP RQ ICP-MS. In the case of Dy/Nd binary synthetic solution, ICP-MS analyses were performed on a Thermo X series II ICP-MS. In the case of PRB leachate breakthrough and non-selective desorption, the elemental composition was determined using an Agilent 7900 ICP-MS. All samples and calibration standards were acidified using concentrated nitric acid (70 wt%, purity ≥99.999% trace metals basis, Sigma-Aldrich) to 2% (v/v), and spiked with internal standards of In, Rh, and Bi to adjust for shifts in signal intensity during analysis. Samples were analyzed in both hydrogen (for Ca and Si) and helium (for all other elements) reaction gas mode to reduce doubly charged and polyatomic interferences. Due to the complex matrix of coal ash leachate, it was necessary to use correction equations to adjust for mass interferences with of ^{45}Sc and ^{153}Eu. A single replicate was used for the column breakthrough tests given the high sampling frequency throughout the breakthrough curves. All feed solutions were performed in triplicate. To describe the experimental uncertainty of metal ion quantification in complex synthetic solutions and leachate solutions, a coefficient of variation for each metal ion concentration was determined based on measurements made in triplicate with feed solutions.

Leaching and pH adjustment of PRB coal ash

Leaching and pH adjustment of PRB coal ash was performed as described previously.[5, 6] Briefly, a PRB coal fly ash sample collected in 2017 from a pulverized coal-fired power plant was leached in 40 mL of a 1 M HCl solution for 4 h at 85 °C at a pulp density of 100 g/L. The leachate was cooled to room temperature and centrifuged at 3000 ×*g* for 15 min to remove any undissolved

particles. The supernatant of the leachate solution was then collected and 10 M NaOH was added dropwise to adjust the pH from 3.8 to 5 (as monitored by a combination pH electrode) to reduce the Fe content via precipitation. The pH-adjusted leachate was centrifuged again to remove precipitates formed during pH adjustment and then filtered using a 0.2 μm polypropylene filter.

SUPPLEMENTAL RESULTS

FT-IR

As shown in the Figure 1, the 1060 cm^{-1} peak was assigned to a glycosidic bond that forms the backbone of the agarose polymer. In the SMCC spectrum, the peaks located at 1200 cm^{-1} and 1706 cm^{-1} were ascribed to succinimide and maleimide groups, respectively. After reaction of amine-functionalized agarose with SMCC, the presence of a 1706 cm^{-1} peak and the lack of a 1200 cm^{-1} peak indicates successful maleimide functionalization. Lastly, after the thiol-maleimide click chemistry, the LanM-agarose spectrum showed two peaks at 1650 cm^{-1} and 1520 cm^{-1}, which correspond to Amide I and Amide II bands from the protein backbone, respectively, supporting immobilization of LanM.

SUPPLEMENTAL TABLES AND FIGURES

Table S1. Metal ion concentration of synthetic feed solution (mM) in **Figure 3**.

	Average	Standard deviation	Coefficient of variation (%)
Na	14.01	0.14	1.00
Mg	3.33	0.07	2.00
Al	9.18	0.09	1.00
Ca	2.32	0.19	8.12
Co	1.93	0.01	0.77
Ni	1.95	0.02	0.87
Cu	1.82	0.02	1.00
Zn	2.13	0.02	1.07
Nd	0.19	0.00	0.86

Table S2. Metal ion concentration of synthetic feed solution (mM) in **Figure S2**.

	Average	Standard deviation	Coefficient of variation (%)
Fe	0.94	0.01	0.86
Nd	0.20	0.00	0.90

Table S3. Metal ion concentration of synthetic feed solution (μM) in **Figure 4** and **Figure S3-5**.

	Average	Standard deviation	Coefficient of variation (%)
50/50 Feed			
Nd	178.92	0.59	0.33
Dy	179.37	0.92	0.51
95/5 Feed			
Nd	337.52	0.92	0.27
Dy	17.63	0.07	0.40
Collected 56/44 Feed			
Nd	26.76	0.23	0.85
Dy	20.93	0.14	0.67

Table S4. Comparison between the LanM column and reported methods for Nd/Dy separation

Type	Method	Solvent or mobile phase	Dy purity		Yield[a]	Experimental conditions	Process requirements and applications	Ref.
			Feed	Product				
Liquid-liquid extraction	Cyanex® 272	Kerosene	6.7%	47.1%	92.3%	Phase ratio 1:1=Aqueous/organic, single stage	Currently used for mass production of REE; compatible with non-REE impurities (may require extra stage with different type of organic ligand);	[7]
	PC88A	Kerosene	16.4 %	74.5%	99%	Phase ratio 1:1=Aqueous/organic, three stages		[8]
	PC88A	Kerosene	16.7 %	94.6%	99%	Phase ratio 1:1.5=Aqueous/organic, four stages		[8]
Crystallization	Chelating tripodal ligand RE(TriNOx)	Benzene	50%	94.6%	90%	Precipitation in benzene	Limited to batch operation; unknown compatibility with non-REE impurities.	[9]
	Borate crystallization	Aqueous	50%	99.0%	>99.9 %	200 °C incubation for 5 days following by cooling for 2 days		[10]
Ion exchange	Chelation ion chromatography	HNO_3 aqueous	13.4 %	>99.9%	>99%	Elution ion exchange	Limited to analytical chemistry or small-scale REE purification.	[11]
	Ligand-assisted displacement chromatography [b]	EDTA+Cu	45%	99.2%	70%	Displacement ion exchange	Comparable productivity to liquid-liquid extraction; unknown compatibility with non-REE impurities.	[12]
Solid-phase extraction	Solvent-impregnated resin	HNO_3 aqueous	16.7 %	99.9%	66%	Pure Dy solution applied as scrubbing process to upgrade product Dy purity	Pre-treatment required for removal of non-REE impurities.	[13]
	LanM column	HCl aqueous	50%	99.9%	76.2%	Two pH-step desorption	Compatible with complex non-REE impurities; adaptable to current adsorption process for continuous operation (i.e. column rotation); improved loading capacity required for scale-up.	This work
		HCl aqueous	5%	46.1%	88.6%	Two pH-step desorption		
		Citrate+HCl aqueous	50%	99.1%	94.2%	Citrate-pH step desorption		
		Citrate+HCl aqueous	5%	50.3%	73.9%	Citrate-pH step desorption		

[a] Yield calculations do not take into account feed recycling.

[b] Only a Nd/Dy separation step (Zone II column A) was used for direct comparison.

Table S5. Metal ion concentration of synthetic feed solution (μM) in **Figure 5**.

	Average	Standard deviation	Coefficient of variation (%)
Y	74.81	0.97	1.30
Nd	255.74	2.36	0.92

Table S6. Metal ion concentration in PRB feed solution (μM) at pH 5.

	Average	Standard deviation	Coefficient of variation (%)
Li	203.010	9.856	4.855
Be	0.963	0.325	33.706
Na	61626.204	989.812	1.606
Mg	80210.044	1178.194	1.469
Al	858.709	16.698	1.945
Si	8.503	0.594	6.980
K	1739.691	32.054	1.843
Ca	273173.440	1477.705	0.541
Sc	0.069	0.009	12.586
V	0.021	0.005	23.876
Mn	157.649	1.738	1.103
Fe	3.990	0.546	13.675
Co	27.054	0.165	0.610
Ni	50.702	0.421	0.830
Cu	94.046	0.577	0.613
Zn	127.133	0.324	0.255
Se	0.151	0.015	10.066
Rb	4.176	0.002	0.043
Sr	2057.752	9.659	0.469
Y	35.326	0.136	0.384
Ba	11.503	0.067	0.582
La	23.636	0.060	0.253
Ce	46.504	0.156	0.336
Pr	6.300	0.027	0.424
Nd	24.453	0.114	0.467
Sm	4.467	0.040	0.892
Eu	0.987	0.003	0.267
Gd	4.188	0.016	0.379
Tb	0.600	0.004	0.692
Dy	3.448	0.020	0.580
Ho	0.648	0.005	0.749
Er	1.780	0.016	0.916
Tm	0.224	0.001	0.279
Yb	1.256	0.020	1.585
Lu	0.185	0.004	1.927
Pb	2.443	0.004	0.151
Th	0.000	0.000	
U	0.030	0.023	77.765

Table S7. Metal ion concentration (μM) in the combined three most concentrated fractions of the PRB desorption solution. The uncertainty for each element was assumed based on the triplicate test from **Table S5**. Note: Compared with the feed composition in Table S5, HREEs (Tb-Lu, Y) are less enriched than LREEs (La-Gd) due to the column being run past the breakthrough point for the presentation of **Figure 5A**.

	Average	Standard deviation	Coefficient of variation (%)
Li	0.011	0.000	0.000
Be	0.000	0.000	
Na	199.627	4.997	2.503
Mg	19.309	0.155	0.804
Al	21.718	0.178	0.821
Si	12.628	0.124	0.979
K	148.153	2.448	1.653
Ca	74.565	0.204	0.273
Sc	0.339	0.001	0.356
V	0.000	0.000	
Mn	1.487	0.007	0.445
Fe	5.206	0.162	3.115
Co	0.000	0.000	
Ni	0.000	0.000	
Cu	0.272	0.000	0.000
Zn	6.660	0.005	0.082
Se	0.092	0.004	3.854
Rb	0.023	0.000	0.030
Sr	0.339	0.001	0.229
Y	10.956	0.026	0.234
Ba	0.000	0.000	
La	177.838	0.564	0.317
Ce	448.001	6.465	1.443
Pr	63.554	0.116	0.183
Nd	247.153	1.892	0.765
Sm	44.894	0.119	0.266
Eu	9.838	0.007	0.075
Gd	36.405	0.063	0.173
Tb	4.307	0.013	0.309
Dy	14.679	0.044	0.302
Ho	1.200	0.005	0.420
Er	1.506	0.007	0.487
Tm	0.067	0.000	0.169
Yb	0.346	0.003	0.874
Lu	0.050	0.000	0.943
Pb	0.000	0.000	
Th	0.000		
U	0.028	0.005	19.369

Table S8. Metal ion concentration (μM) in the PRB leachate feed, and three desorption zones in **Figure 5E and 5F**.

	Feed			Front	Middle	Rear
	Average	Standard deviation	Coefficient of variation (%)			
Li	221.220	8.278	3.742			
Be	1.247	0.057	4.530			
Na	83262.588	2974.199	3.572			
Mg	84478.993	2756.163	3.263	5.246	0.743	0.044
Al	981.596	22.688	2.311	10.474	2.076	1.725
K	1910.022	55.005	2.880			
Ca	126773.564	3260.582	2.572	7.645	1.500	1.030
Sc	0.021	0.000	1.089	0.012	0.009	0.045
Ti	546.018	13.212	2.420	0.318	0.290	0.291
V	0.009	0.000	1.530			
Cr	0.028	0.001	3.869	0.015	0.015	0.100
Mn	165.665	3.303	1.994	0.044	0.024	0.019
Fe	3.011	0.128	4.244	1.103	0.644	0.889
Co	26.208	0.119	0.455	0.003	0.000	0.001
Ni	48.771	0.689	1.413	0.375	0.012	0.043
Cu	82.732	1.478	1.786	1.977	0.122	0.108
Zn	107.892	1.259	1.167	0.226	0.214	0.236
Se	2.799	0.050	1.784	1.977	3.010	7.355
Rb	4.641	0.009	0.193	0.120	0.033	0.002
Sr	1929.365	4.871	0.252	0.684	0.076	0.032
Y	34.502	0.176	0.510	77.459	13.651	0.152
Cd	0.755	0.001	0.157	0.000		0.001
Cs	0.218	0.002	1.021	0.000		0.000
Ba	11.581	0.101	0.868	0.007	0.011	0.005
La	25.551	0.087	0.341	16.677	23.929	41.284
Ce	49.069	0.229	0.468	11.680	17.585	115.726
Pr	6.230	0.023	0.375	0.860	1.316	15.781
Nd	21.673	0.110	0.508	2.696	4.208	55.799
Sm	4.328	0.036	0.828	0.334	0.556	10.439
Eu	1.145	0.005	0.447	0.173	0.283	2.445
Gd	4.266	0.016	0.370	2.425	3.680	6.761
Tb	0.645	0.003	0.409	0.606	0.794	0.701
Dy	3.490	0.020	0.559	4.891	4.736	1.738
Ho	0.690	0.004	0.560	1.311	0.773	0.084
Er	1.835	0.008	0.460	3.951	1.257	0.071
Tm	0.235	0.002	0.665	0.579	0.078	0.001
Yb	1.243	0.005	0.428	2.943	0.211	0.016
Lu	0.189	0.003	1.410	0.457	0.013	0.004
Pb	2.165	0.024	1.113	0.749	0.004	0.002
U	0.024	0.000	1.049	0.057	0.002	0.002

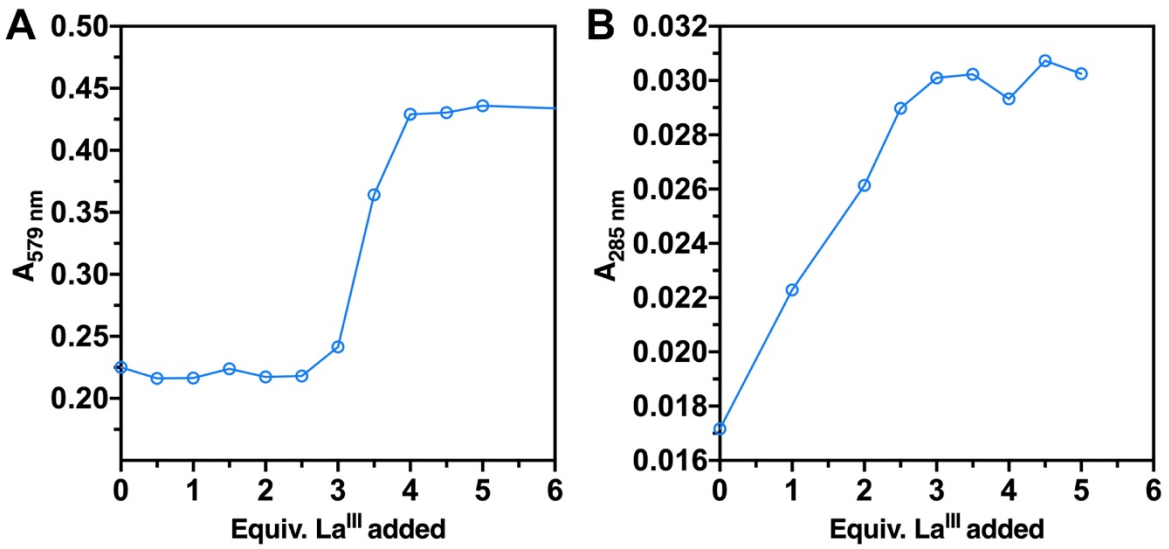

Figure S1. Stoichiometric titrations of LanM-Cys with La(III) demonstrate binding of 3 equiv. of REEs. A) Competative titration using xylenol orange as an indicator, performed in Chelex-treated 20 mM MES, 100 mM KCl, pH 6.0. B) The conformational response of LanM to La(III) can be tracked as a shift in the A_{285nm}. Titration performed in Chelex-treated 30 mM MOPS, 100 mM KCl, pH 7.0.

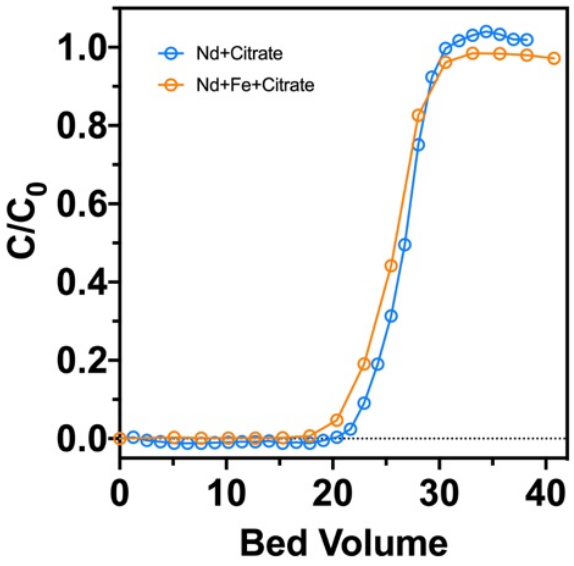

Figure S2. Nd breakthrough curves in the presence and absence of Fe^{3+}. Feed: Nd+Citrate: 0.2 mM Nd, 20 mM citrate, pH 3; Nd+Fe+Citrate: 0.2 mM Nd, 0.9 mM Fe, 20 mM citrate, pH 3.

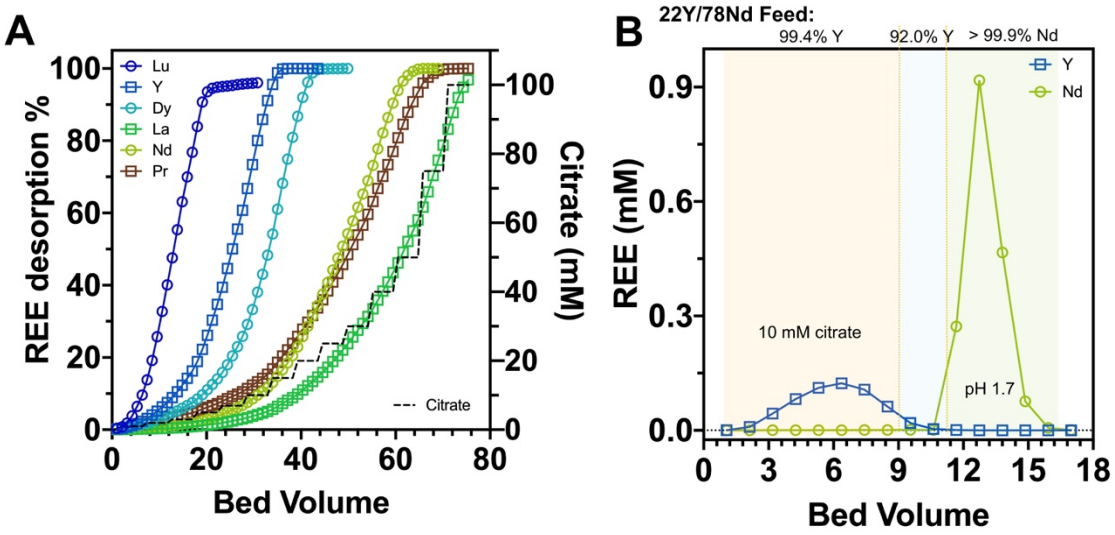

Figure S3. (A) Accumulative desorption profiles of single-element independently loaded columns using a stepwise citrate concentration (pH 5) scheme; (B) A feedstock comprising a 22:78 mixture of Y:Nd was loaded to 75% column saturation and then subjected to a two-step desorption scheme using 10 mM citrate (pH 5, bed volumes 1-10) followed by pH 1.7. The values above each panel indicate the purity of REE over each elution zone divided by vertical dot lines. The detailed feed composition and measurement uncertainty are listed in **Tables S3 and S5**. 1 bed volume = 0.94 mL.

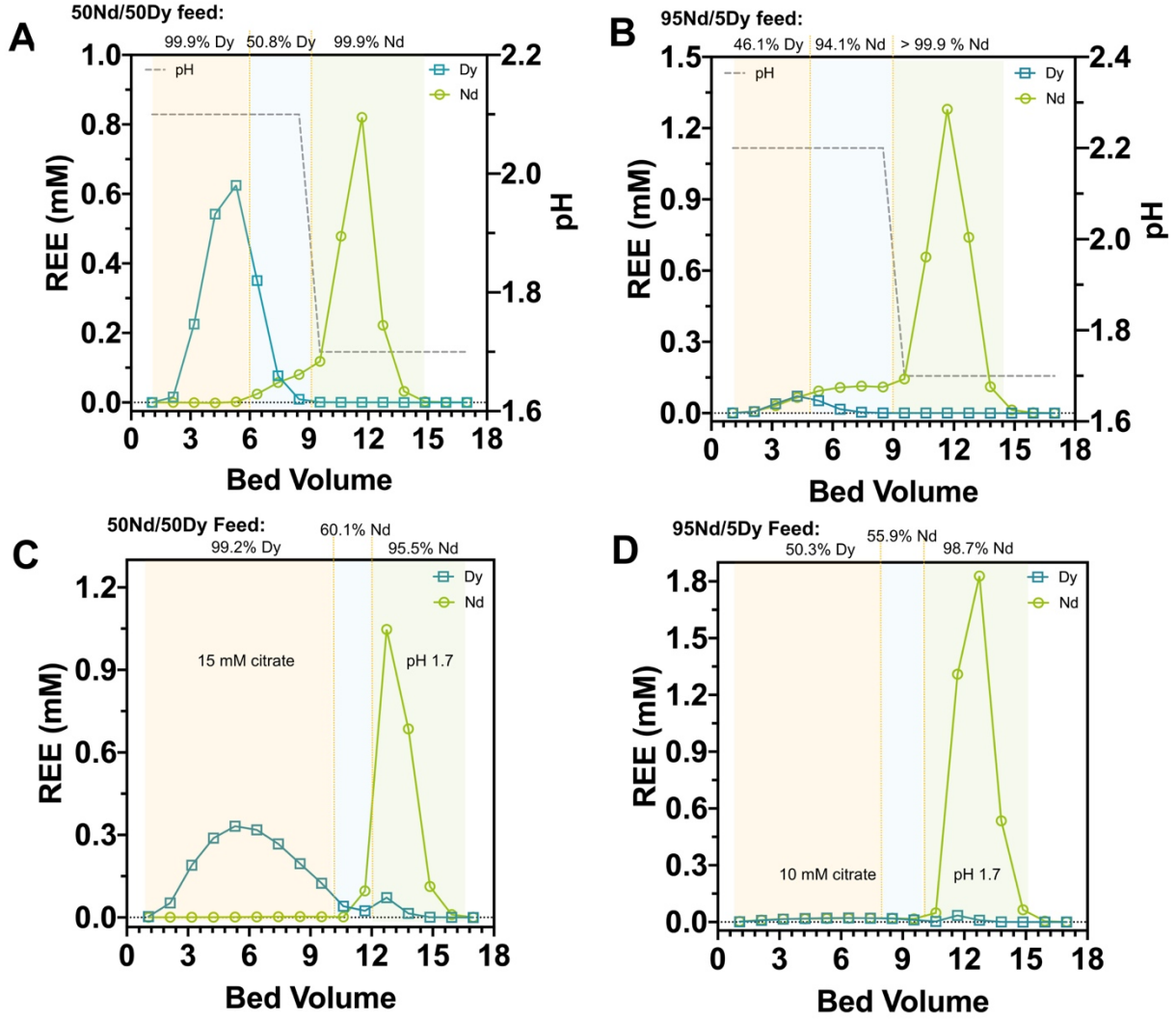

Figure S4. Dy/Nd separation using a two-pH and pH-citrate desorption scheme. The values above each panel indicate the purity of REE over each elution zone divided by vertical dotted lines (yellow). The duration of each pH step is depicted by the gray dashed line. Experimental conditions: REE solutions at pH 3 were used to load the column to 75% saturation; Feed composition: (A) and (C) Dy:Nd=50:50, (B) and (D) Dy:Nd=5:95. Desorption condition: (A) pH 2.1 and pH 1.7, (B) pH 2.2 and pH 1.7, (C) 15 mM citrate (pH 5, bed volumes 1-10) and pH 1.7, and (D) 10 mM citrate (pH 5, bed volumes 1-10) and pH 1.7. The detailed feed composition and measurement uncertainties are listed in **Table S3** and **Table S5**. 1 bed volume = 0.94 mL.

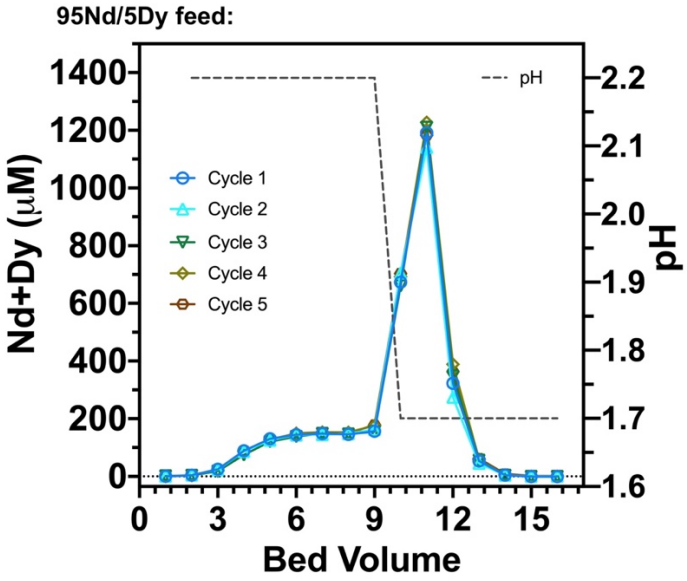

Figure S5. In order to perform a coupled two-step desorption (**Figure 4E** and **F**), a feedstock comprising a 5:95 mixture of Dy:Nd was subjected to 5 cycles of a two-step pH desorption scheme. The individual Nd and Dy concentrations for cycle 1 were measured by ICP-MS as shown in **Figure 4E**. The total REE (Nd+Dy) concentrations for each cycle were quantified using an Arsenazo III assay and plotted here. 1 bed volume = 1 mL. The collected desorption profiles are almost identical, suggesting the high reproducibility of the column experiments

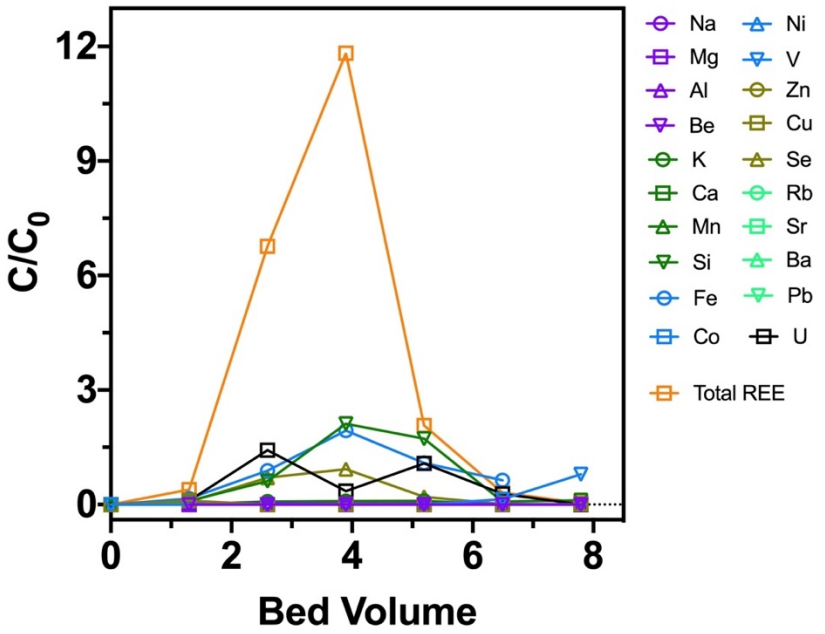

Figure S6. Desorption profiles of a Powder River Basin (PRB) fly ash leachate using the LanM agarose column. Experimental conditions: 35 bed volumes of PRB fly ash leachate was pumped through a 0.8 mL column, followed by a washing step with 5 bed volumes of pH 3.5 water. Desorption was performed with 10 bed volumes of pH 1.5 HCl.

REFERENCES

1. Cotruvo, J. A.; Featherston, E. R.; Mattocks, J. A.; Ho, J. V.; Laremore, T. N., Lanmodulin: A Highly Selective Lanthanide-Binding Protein from a Lanthanide-Utilizing Bacterium. *Journal of the American Chemical Society* **2018,** *140* (44), 15056-15061.
2. Featherston, E. R.; Mattocks, J. A.; Tirsch, J. L.; Cotruvo, J. A., Chapter Six - Heterologous expression, purification, and characterization of proteins in the lanthanome. In *Methods in Enzymology*, Cotruvo, J. A., Ed. Academic Press: 2021; Vol. 650, pp 119-157.
3. Dong, Z.; Deblonde, G.; Middleton, A.; Hu, D.; Dohnalkova, A.; Kovarik, L.; Qafoku, O.; Shutthanandan, V.; Jin, H.; Hsu-Kim, H.; Theaker, N.; Jiao, Y.; Park, D., Microbe-Encapsulated Silica Gel Biosorbents for Selective Extraction of Scandium from Coal Byproducts. *Environ Sci Technol* **2021,** *55* (9), 6320-6328.
4. Deblonde, G. J. P.; Mattocks, J. A.; Park, D. M.; Reed, D. W.; Cotruvo, J. A.; Jiao, Y., Selective and Efficient Biomacromolecular Extraction of Rare-Earth Elements using Lanmodulin. *Inorg Chem* **2020,** *59* (17), 11855-11867.
5. Park, D.; Middleton, A.; Smith, R.; Deblonde, G.; Laudal, D.; Theaker, N.; Hsu-Kim, H.; Jiao, Y., A biosorption-based approach for selective extraction of rare earth elements from coal byproducts. *Separation and Purification Technology* **2020,** *241*, 116726.
6. Middleton, A.; Park, D. M.; Jiao, Y.; Hsu-Kim, H., Major element composition controls rare earth element solubility during leaching of coal fly ash and coal by-products. *International Journal of Coal Geology* **2020,** *227*, 103532.
7. Sun, P.-P.; Kim, D.-H.; Cho, S.-Y., Separation of neodymium and dysprosium from nitrate solutions by solvent extraction with Cyanex272. *Minerals Engineering* **2018,** *118*, 9-15.
8. Yoon, H. S.; Kim, C. J.; Chung, K. W.; Kim, S. D.; Kumar, J. R., Process development for recovery of dysprosium from permanent magnet scraps leach liquor by hydrometallurgical techniques. *Canadian Metallurgical Quarterly* **2015,** *54* (3), 318-327.
9. Bogart, J. A.; Lippincott, C. A.; Carroll, P. J.; Schelter, E. J., An Operationally Simple Method for Separating the Rare-Earth Elements Neodymium and Dysprosium. *Angewandte Chemie International Edition* **2015,** *54* (28), 8222-8225.
10. Yin, X.; Wang, Y.; Bai, X.; Wang, Y.; Chen, L.; Xiao, C.; Diwu, J.; Du, S.; Chai, Z.; Albrecht-Schmitt, T. E.; Wang, S., Rare earth separations by selective borate crystallization. *Nature Communications* **2017,** *8* (1), 14438.
11. Ashour, R. M.; Samouhos, M.; Polido Legaria, E.; Svärd, M.; Högblom, J.; Forsberg, K.; Palmlöf, M.; Kessler, V. G.; Seisenbaeva, G. A.; Rasmuson, Å. C., DTPA-Functionalized Silica Nano- and Microparticles for Adsorption and Chromatographic Separation of Rare Earth Elements. *Acs Sustain Chem Eng* **2018,** *6* (5), 6889-6900.
12. Ding, Y.; Harvey, D.; Wang, N.-H. L., Two-zone ligand-assisted displacement chromatography for producing high-purity praseodymium, neodymium, and dysprosium with high yield and high productivity from crude mixtures derived from waste magnets. *Green Chem* **2020,** *22* (12), 3769-3783.
13. Yamada, E.; Murakami, H.; Nishihama, S.; Yoshizuka, K., Separation process of dysprosium and neodymium from waste neodymium magnet. *Separation and Purification Technology* **2018,** *192*, 62-68.